A paramaterization for the absorption due to the near infrared bands of CO_2

By J. T. KIEHL, CHR. BRÜHL[1] and TAKASHI YAMANOUCHI[2], *National Center for Atmospheric Research*[3], *P.O. Box 3000, Boulder, Colorado 80307, USA*

ABSTRACT

A broad band absorption parameterization for the near-infrared bands of CO_2 is described. This parameterization is in excellent agreement with more detailed line-by-line calculations for a large range of pressures, temperatures and amounts of CO_2. The role of near IR absorption due to CO_2 is investigated for the earth's atmosphere. It is shown that the presence of these near-IR absorption bands contributes to a heating of nearly 0.2 K/day in the upper stratosphere and 0.05 K/day in the lower stratosphere. Although the magnitude of heating in the lower stratosphere is small, it contributes more heating than ozone near the tropical tropopause region.

1. Introduction

Accurate methods for calculating short wave < 4 μm absorption of solar radiation by H_2O, CO_2, and O_3 are necessary for evaluating accurate heating rates in the atmosphere, especially in the region of the lower stratosphere where the total net radiative heating is as small as 0.1–0.3 K day^{-1}. Houghton (1978) has pointed out that the lower stratosphere net radiative heating is the sum of a number of very small contributions arising from heating and cooling due to a number of constituents. He also stressed the need for "accurate calculations" of these individual components. Carbon dioxide has a number of absorption bands in the near infrared (IR) region which are effective in absorbing incoming solar radiation. The introduction of the absorption due to these near IR bands in climate models necessitates the development of an accurate and computationally fast method. Over the past 20 years, a number of methods have appeared which can be used to calculate the heating due to the

near-IR bands of CO_2. In particular, Yamamoto (1962) employed the data of Howard et al. (1955) to calculate the absorption due to these bands. Houghton (1963) employed the data of Burch et al. (1960a, b) to formulate expressions for the absorptance for the individual bands of CO_2. Sasamori et al. (1972) fit Burch et al.'s (1960a, b) data to obtain an expression for the fractional absorption due to the combination of all of the CO_2 bands. Finally, Raschke and Stucke (1973) derived exponential sum-fit coefficients (see Wiscombe and Evans (1977) for a complete description of this method) by fitting the data of Howard et al. (1956). It is evident that all of these methods have employed the data from Howard and Burch's efforts. More recently, Tanaka and Yamanouchi (1977) have carried out extensive measurements and detailed line-by-line calculations on the absorption properties of the 1.4, 1.6, 2.0, 2.7, 4.8, and 5.2 μm band systems of CO_2. Tanaka and Yamanouchi (1977) also compared their measured absorptances with the formulae derived by Howard et al. (1955). They found substantial discrepancies between their measurements and the formula of Howard et al. for the 1.4 and 1.6 μm bands and for low CO_2 amounts for the 2 μm band. Yamanouchi (1977) presents tables of fractional absorptance

---

[1] Max Planck Institut für Chemie, Mainz, FRG.
[2] National Institute of Polar Research, Tokyo, Japan.

from line-by-line calculations for each of these bands for a large range in total pressure and amount of CO_2 and three temperatures. The present work employs the results of Yamanouchi (1977) to construct a broadband model for each of the 1.4, 1.6, 2.0, 2.7 μm band systems. The 4.8 and 5.2 μm bands are much weaker and very little solar energy is available in this spectral region. The 4.3 μm band system model is evaluated by using data from Burch et al. (1962) since Yamanouchi (1977) did not perform calculations or measurements for this band.

Section 2 discusses the formulation of the broadband absorptance model used for the near-infrared bands. The relative error between the line-by-line calculations and the broadband model for each individual band is presented with a discussion on the possible sources of error. Section 3 discusses the application of the broadband model in evaluating the atmospheric heating due to each of the near infrared bands. Finally, results for heating due to a doubling and quadrupling of atmospheric CO_2 are presented.

2. The broad band model

The broad band absorptance model is based on the formulation described in Kiehl and Ramanathan (1983). The absorptance (or equivalent width) for each band system is defined by:

$$A = 2A_0(\bar{T}) \sum_j \tau_j \ln\left\{1 + \sum_k u_k\right.$$
$$\left.[4 + u_k(1 + 1/\beta_k)]^{-1/2}\right\}. \tag{1}$$

The sum over k under the logarithm accounts for closely neighboring, totally overlapped bands. The sum over j accounts for bands which are separated but may be overlapped by the wings of the stronger bands. The totally overlapped bands are isotopic and "hot" bands as listed in Table 1 and are denoted by k. Isotopic hot bands with strengths less than 0.00072 cm^{-2} atm^{-2} are neglected. The dimensionless optical pathlength is:

$$u_k = \frac{c}{\mu} \int_{P_1}^{P_2} \frac{S_k H(T)}{A_0(T)} \, dP, \tag{2}$$

and the mean line parameter is:

$$\beta_k = \frac{4}{d_k u_k} \int_{P_1}^{P_2} \gamma(T) \frac{P}{P_0} \, du_k, \tag{3}$$

where $S_k(T)$ (cm^{-2} atm^{-1}) is the band strength for band k (see Table 1). The temperature dependence of the band is given in Kiehl and Ramanathan (1983). The temperature dependence due to the Boltzmann factor for the hot bands, stimulated emission and the vibrational partition function are explicitly taken into account. c is the volume mixing ratio of CO_2 (320 ppmv), μ is the cosine of the solar zenith angle. $H(T)$ is the atmospheric scale height (cm), P is the total atmospheric pressure (atm), and $A_0(T)$ is the effective bandwidth (cm^{-1}). In eq. (1), A_0 is evaluated for a pressure weighted temperature along the path. $A_0(T)$ is determined from fitting the broad-band model to either laboratory data or detailed line-by-line calculations. The temperature dependence of A_0 accounts for effective increase in the bandwidth due to the excitation of higher rotational states at higher temperatures. d_k (cm^{-1}) is the mean line spacing (see Table 1) and $\gamma(T)$ is the mean line half width (cm^{-1}). τ_j is the transmission function of the wings of the strongest bands in this region and is given by:

$$\tau_j = \frac{1}{1 + u_j^{eff} [4 + u_j^{eff} (1 + 1/\beta_j)]^{-1/2}} \tag{4}$$

where

$$u_j^{eff} = \frac{c}{\mu} \int_{P_2}^{P_1} \frac{S_j^{eff}}{A_0(T)} H(T) \, dP. \tag{5}$$

S_j^{eff} is defined in (7) and its evaluation is discussed after eq. (7).

The value of γ for nitrogen broadend lines which is used for the near-IR bands is the same as that employed by Kiehl and Ramanathan (1983) for the 15 μm band:

$$\gamma(T) = 0.067 (300/T)^{2/3} \text{ cm}^{-1}. \tag{6}$$

This value of γ is in agreement with measurements of Boldyrev and Vasilevskii (1973) for the 1.6 μm band and of Tubbs and Williams (1972) for the 4.3 μm and Vasilevskii et al. (1975) for the 2.0 μm band. A more detailed description of (1) and the band parameters can be found in Kiehl and Ramanathan (1983).

The CO_2 bands employed in the present study are listed in Table 1. The band strengths are taken from Rothman and Young (1981) and the band positions are from Rothman et al. (1983). Yamanouchi (1977) employed the band strengths of Tanaka and Yamanouchi (1977) for the line-

Table 1. *Band parameters used in the broad band model for near IR CO$_2$ absorption*

Region (μm)	Type	Transition			j	k	Bandcenter (cm^{-1})	Strength* at 273 K (cm^{-2} atm^{-2})	Mean Line Spacing (cm^{-1})
		Isotope	lower	upper					
1.4	M	626	00^00_1	00^03_1	1		6972.579	0.04023	1.56
		626	01^10_1	01^13_1	2		6935.136	0.00304	0.78
1.6	C	626	00^00_1	30^01_1	1		6503.084	0.00134	1.56
		626	01^10_1	31^11_2	2		6356.299	0.00088	0.78
		626	00^00_1	30^01_2	3		6347.855	0.01149	1.56
		626	00^00_1	30^01_3	4		6227.920	0.01149	1.56
		626	01^10_1	31^11_3	5		6196.180	0.00072	0.78
		626	00^00_1	30^01_4	6		6075.984	0.00122	1.56
2.0	C	626	01^10_1	21^11_1	1	1	5123.195	0.286	0.78
		626	00^00_1	20^01_1		2	5099.659	0.302	1.56
		636	00^00_1	20^01_1	2	1	4991.353	0.0057	1.56
		626	00^00_1	20^01_2		2	4977.837	0.941	1.56
		626	01^10_1	21^11_2		3	4956.381	0.0714	0.78
		636	00^00_1	20^01_2	3		4887.387	0.0080	1.56
		626	00^00_1	20^01_3	4		4853.625	0.217	1.56
		626	01^10_1	21^11_3	5		4807.697	0.0180	0.78
2.7	C	626	01^10_1	11^11_1	1		3723.249	3.05	0.78
		626	00^00_1	10^01_1	2		3714.783	40.35	1.56
		636	00^00_1	10^01_1	3		3632.911	0.43	1.56
		626	00^00_1	10^01_2	4		3612.842	27.84	1.56
		626	01^10_1	11^11_2	5		3580.326	2.16	0.78
		636	00^00_1	10^01_2	6		3527.737	0.25	1.56
4.3	F	636	01^10_1	01^11_1	1		2271.760	2.198	0.78
		636	00^00_1	00^01_1	2		2283.488	25.798	1.56
		626	02^20_1	02^21_1	3	1	2324.141	8.275	0.78
		626	10^00_1	10^01_1		2	2326.598	3.178	1.56
		626	10^00_2	10^01_2		3	2327.433	5.196	1.56
		628	00^00_1	00^01_1	4	1	2332.113	8.947	0.78
		626	01^10_1	01^11_1		2	2336.633	205.80	0.78
		626	00^00_1	00^01_1	5		2349.143	2578.7	1.56

* Hot band population factor at room temperature of 296K included.
The abbreviations M, C, F stand for multiple, combination and fundamental bands, respectively.
The isotope code gives the last digit of the mass number of each atom.
The band positions are taken from Rothman et al. (1983), the band strengths from Rothman and Young (1981).

by-line calculations. Tanaka and Yamanouchi (1977) employed band strengths which were determined from their own laboratory measurements. These band strengths differ from those listed in Table 1. Since the present calculations employ the line-by-line results of Yamanouchi (1977) to obtain A_0, the effective bandwidth parameter, the broad band model should also use the band strengths of Tanaka and Yamanouchi (1977). The band strengths of Rothman and Young (1981) have therefore been renormalized to agree with Tanaka and Yamanouchi (1977). The ratios of these band strengths are given in Table 2.

Table 2. *The ratios of Tanaka and Yamanouchi's (1977) band strengths to Rothman and Young's (1981) values*

Spectral region (μm)	1.4	1.6	2.0	2.7
$S_{Yamanouchi}/S_{Rothman}$	1.0000	1.1422	1.0995	1.0012

Only the bands in Table 1 denoted by k are assumed to be completely overlapped. In the other cases, either partial or no-overlap takes place. Only the 2.7 and 4.3 μm bands in (1) require a τ_j which is not equal to 1. For the 2.7 μm band system, the

wings of both the $00° 0_1-10° 1_1$, and $00° 0_1-10° 1_2$ bands overlap the weaker bands. Thus, τ_j for this band system is a product of the transmission factor for each of these two strong bands. To determine the transmissivity factor, the intensity distribution of the lines for the bands is needed. Previously, for the 15 μm band, an exponential distribution was assumed for the lines. For the near-infrared bands, there is no Q branch present. In the presence of just the P and R branches, the line intensities for a rigid rotor are distributed with a gaussian shape. To find the appropriate line intensity distribution for the band wings, the expression for the distribution of rotational line strengths (Steinfeld, 1974) was used to calculate the intensity of overlapping Lorentzian lines in the band as a function of the distance from the band center. This intensity distribution was then smoothed and fit by a simple expression for distances between 20 and 120 cm^{-1} from the band center. The effective intensity of the band wings is given by:

$$S_j^{\text{eff}} = \frac{0.7168\,A_0^5\,S_j}{|v - v_0|^5 + 0.7168 A_0^5},\qquad (7)$$

where v_0 is the band center. It should be noted that a functional form of $\text{Exp}[-(v - v_0)^2]$, which is in agreement with theoretical arguments, was also assessed for S_j^{eff}. However, it was found that (7) yielded much better agreement with the line-by-line absorptances. Deviations from the gaussian wing shape are realistic, and are due to asymmetries in the molecular potential (Galtsev and Tsukanov, 1979). It should also be pointed out that the individual lines may be sub-Lorentzian in shape. However, for nearly all the absorptances used in the following calculations, the effect of non-Lorentzian line shapes is negligible. This has been confirmed by the study of Tanaka and Yamanouchi (1977). Thus, the functional form of (7) is based on its phenomenological value for fitting the line-by-line absorptance. S_j^{eff} depends on the distance between the strongest band in the system and the band which is overlapped by the wing of this strong band. For example, for the 4.3 μm band system, the strongest band is located at $v_0 = 2349.143$ cm^{-1} (see band $j = 5$ in Table 1). To calculate S_j^{eff} for the $j = 4$ band, the band center of $v = 2332.113$ cm^{-1} is used. Thus, $|v - v_0| = 17.03$ cm^{-1} in eq. (7).

With the band intensities, mean line spacing and mean line width determined from spectroscopic

data, the only parameter left to specify is the effective bandwidth, A_0. For the 4.3 μm fundamental and the 1.4 μm multiple band, A_0 was chosen to be the same as that used for the 15 μm band:

$$A_0(T) = 20.38\,(T/250)^{1/2}\,\text{cm}^{-1}\qquad (8)$$

For the combination bands, 1.6, 2.0, and 2.7 μm, it was necessary to find a new A_0. The value of A_0 was obtained by minimizing the difference between the absorptances of Yamaouchi (1977) and the broad band model for a wide range of amounts of CO_2, as well as various total pressures and temperatures. For the combination bands, the best value of A_0 found was:

$$A_0(T) = 25.0\,(T/250)^{1/2}\,\text{cm}^{-1}.\qquad (9)$$

The relative differences between the broad band model and Yamanouchi's line-by-line calculations are presented in Fig. 1–4. Yamanouchi did not calculate the absorptance of the 4.3 μm band. Comparison of the broad band model with the data of Burch et al. (1962) for this band shows good agreement. For relevant present day atmospheric amounts of CO_2, the differences are less than $\pm 10\%$. fig. 1–4 indicate that good agreement exists between the two methods for most amounts and pressures. For the current total column amount of atmospheric CO_2, 300 cm-atm, the errors are less than $\pm 5\%$. In particular, for the combination bands this may seem reasonable since A_0 was adjusted to minimize the differences. However, this might not be the case since only the numerical coefficient of A_0 was changed for these bands. Thus, the good agreement between the models for such large ranges in pressure, temperature and amount is not guaranteed.

The differences between the line-by-line and broad band absorptances can be ascribed to a number of assumptions in the broad band approach. First, in calculating the band wing transmission function it was assumed that the P and R branches were symmetrical. In fact, data indicate that there are asymmetries in these two branches (Galtsev and Tsukanov, 1979). This assumption would most strongly affect the 2.7 and 4.3 μm bands. Second, the fact that these bands do not possess a Q-branch will affect the mean line half width, since this band parameter is obtained by weighting the rotational line half widths with the strengths. This implies that the value of β is
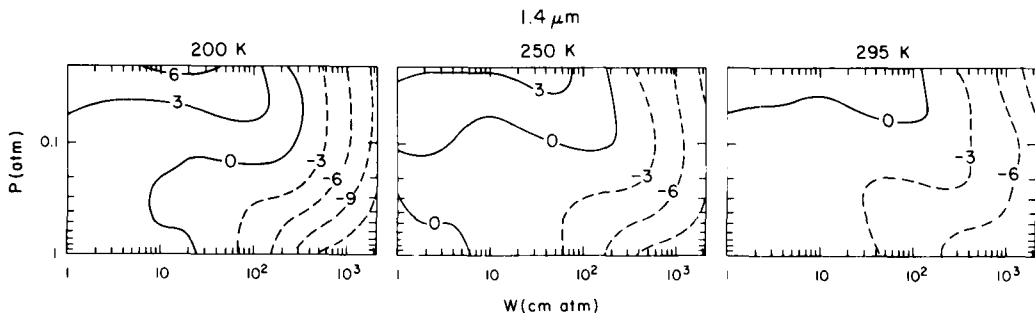
1.4 μm

Fig. 1. % difference between absorptances of the broad band model (1) and the line-by-line results of Yamanouchi (1977) as a function of total pressure and amount of CO_2 (om-atm) for the 1.4 μm CO_2 band at: (a) 200 K, (b) 250 K, (c) 295 K.
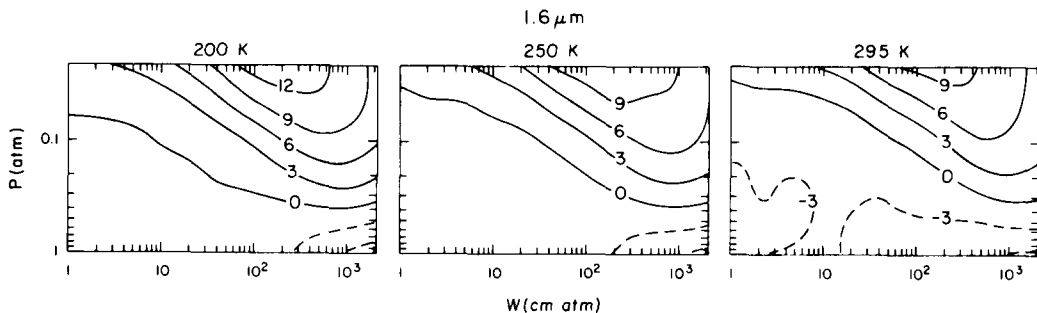
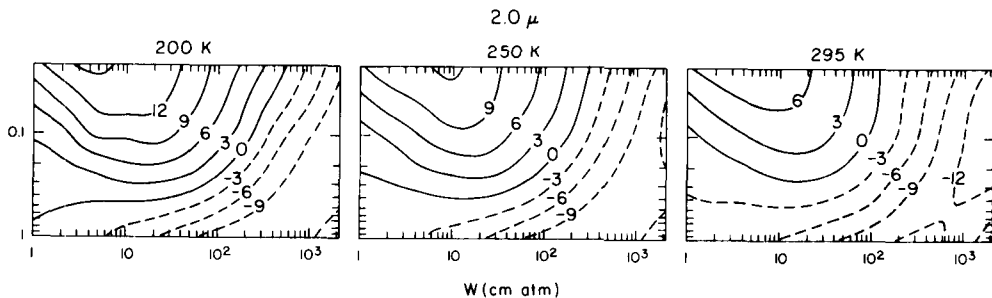1.6 μm

Fig. 2. Same as Fig. 1 but for the 1.6 μm band.

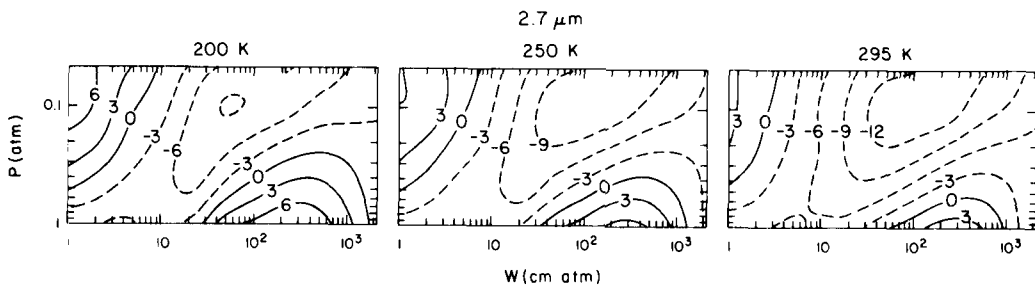2.0 μ

Fig. 3. Same as Fig. 1 but for the 2.0 μm band.

2.7 μm

Fig. 4. Same as Fig. 1 but for the 2.7 μm band.

different for each of the band systems. No attempt was made to recalculate these parameters from the line data; however, calculations were carried out where A_0 was not altered from (7) but γ/d was varied to minimize the differences between the line-by-line results and the broad band absorptances. The results of these calculations implied that (i) a different β would be necessary for each combination band and (ii) even with these different value of β, substantial differences persisted between the band model with the new value of β and the line-by-line results. For example, the maximum % error for the 2.0 μm band system with the new value of a β ranged from -15.0 to 22% for a temperature of 250°K. This should be compared with the range of % difference shown in Fig. 3b of -12 to $+12$%. Therefore, γ/d was fixed for all the bands.

The temperature dependence of the band-strengths in the near-IR bands can be substantial. If this dependence is neglected for the 1.4 and 1.6 μm bands, even the sign of dA/dT is incorrect. Similarly, neglecting the temperature dependence of A_0 can lead to substantial errors.

3. Near-infrared CO_2 heating

To assess the rôle of the near-IR CO_2 bands in atmospheric heating, the broad band absorptances described in Section 2 were incorporated into the radiation model of Ramanathan and Dickinson (1979) using the method of Lacis and Hansen (1974). The overall computational time for the new method requires only 1% of the total model time. Fig. 5 presents the change in heating rates due to the individual near-IR bands along with their total for a latitude of 30N averaged over the months of March, April and May. The 1.4 and 1.6 μm bands are an order of magnitude smaller than the 2.0 μm band and, hence, do not appear in the figure. Thus, these bands contribute negligible heating for present day amounts of CO_2 ($\sim$300 cm-atm). However, for large amounts of CO_2 they can become important. Above 27 km, the 4.3 μm band dominates in radiative heating. Below 27 km, the effect of the strong 4.3 μm band has saturated and the 2.7 μm band contributes more to the heating than the 4.3 μm band. The 4.3 μm band contributes half of the total heating at all heights. The maximum heating due to all of the CO_2 bands occurs at 46
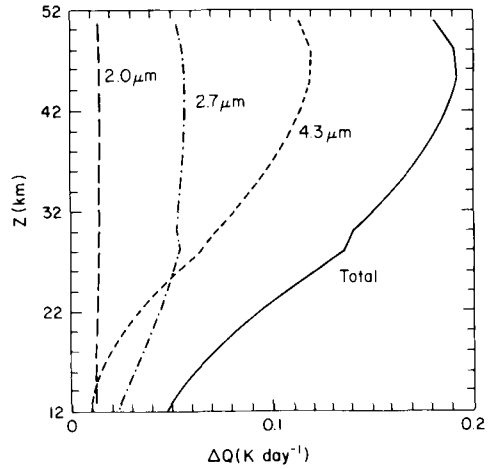

Fig. 5. Near-IR heating due to individual and total CO_2 bands for 30N spring conditions.
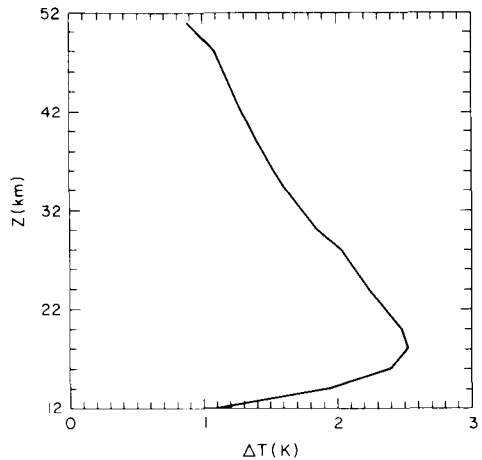

Fig. 6. Change in stratosphere temperatures due to near-IR CO_2 bands for 30N spring conditions.

km with a magnitude of 0.19 K day^{-1}; however, at this height, O_3 heating is roughly 50 times larger.

The temperature change due to the near-IR CO_2 heating at a latitude of 30N averaged for the months of March, April and May (spring conditions) is shown in Fig. 6. Temperatures are calculated for various latitudes using the fixed dynamical heating assumptions described in Ramanathan and Dickinson (1979). The important feature is the height and magnitude of the temperature change. The maximum heating due to CO_2

is located at 46 km, while the maximum temperature change due to the CO$_2$ heating occurs at 18 km. This results from the dependence of radiative relaxation times on height (see Ramanathan et al., 1983). For the fixed dynamical heating model used in this study, the radiative relaxation time near 50 km is approximately 5–7 days, while near 12 to 18 km, the relaxation time is more on the order of 40–50 days. This feature of the lower stratosphere necessitates accurate heating rate calculations. Thus, an error of 0.05 K day^{-1} in net heating in this region would result in errors in temperature on the order of ~2 K. It is important to note that these radiative relaxation times are appropriate for this particular model. Ramanathan et al. (1983) find an even larger relaxation time for the tropopause region, roughly 100 days. This larger relaxation time would imply more sensitivity to the solar CO$_2$ bands. The relative importance of near-IR CO$_2$ heating to heating due to O$_3$ and O$_2$ has been calculated by Kiehl and Yamanouchi (1985). They find that for the tropics below ~20 km, the heating due to CO$_2$ is larger than the heating due to O$_3$ or O$_2$.

The climatic importance of the near-IR CO$_2$ bands has been assessed by employing the one-dimensional radiative-convective model of Ramanathan (1976). The model contains one level of cloud with a fractional amount fixed at 0.49 at a height of 5 km. Neglecting the near-IR CO$_2$ bands results in a 0.34% increase in the planetary albedo

for fixed water vapor amount. It also results in a decrease of surface temperature of 0.4 K for fixed water vapor or 0.8 K for fixed relative humidity. In the latter case, the planetary albedo is 0.4% larger.

The importance of the near-IR CO$_2$ bands to heating due to increased atmospheric CO$_2$ is shown in Fig. 7. These results indicate that neglecting the effects of increased heating by the near-IR CO$_2$ bands would lead to an underestimate of stratospheric temperatures by 0.5–1.°K.

4. Summary

An accurate and computationally fast method for calculating the absorption properties of the near-infrared CO$_2$ bands has been presented. This method is based on the broad band model described in Kiehl and Ramanathan (1983) and Ramanathan (1976). Comparison of the broad-band absorptances with the detailed line-by-line calculations of Yamanouchi (1977) show very good agreement for a large range of pressures and amounts of CO$_2$ for individual bands. The broad band model explicitly accounts for the temperature dependence of the "hot" and isotopic bands.

The near-infrared CO$_2$ bands contribute up to nearly 0.2 K day^{-1} heating at midlatitudes in the upper stratosphere, and 0.05 K day^{-1} heating in the lower regions of the stratosphere. Errors in heating rates of the order of 0.02–0.05 K/day in the lower stratosphere would imply 1–2 K temperature errors in this region. Thus, much care must be exercised in constructing accurate methods for evaluating absorption in this region.
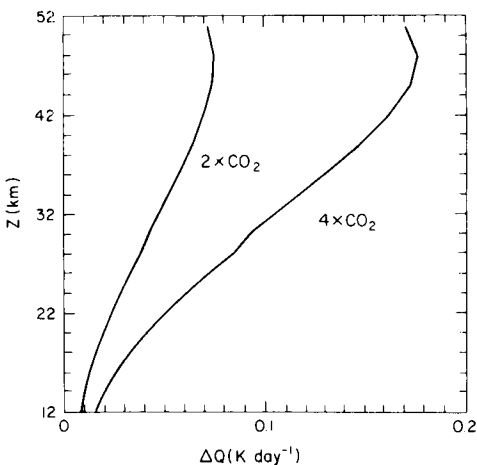
5. Acknowledgements

Fig. 7. Stratospheric heating due to doubling and quadrupling CO$_2$.

REFERENCES

Boldyrev, V. A. and Vasilevskii, K. P. 1973. Intensity and halfwidths of CO_2 lines in the 1401–0000 band. *Opt. Spectrosc. (USSR)* 35, 476–478.

Burch, D. E., Gryvnak, D. and Williams, D. 1960a. Infra-red absorption by carbon-dioxide. Report, Ohio State Univ.

Burch, D. E., Singleton, E. B., France, W. L. and Williams, D. 1960b. Infra-red absorption by minor atmospheric constituents, Report, Ohio State Univ.

Burch, E. E., Gryvnak, D. A. and Williams, D. 1962. Total absorption of carbon dioxide in the infrared. *Appl. Opt. 1*, 759–765.

Galtsev, A. P. and Tsukanov, V. V. 1979. Calculation of the form of the vibrational-rotational absorption bands of carbon dioxide by statistical modeling. *Opt. Spectrosc. (USSR) 46*, 260–273.

Houghton, J. T. 1963. The absorption of solar infra-red radiation by the lower stratosphere *Q. J. R. Meteorol. Soc. 89*, 319–331.

Houghton, J. T. 1978. The stratosphere and mesosphere. *Q. J. R. Meteorol. Soc. 104*, 1–29.

Howard, J. N., Burch, D. E. and Williams, D. 1955. Near-infrared transmission through synthetic atmospheres. *Geophys. Res. Pap.* No. 40, AFCRC-TR-55-213.

Howard, J. N., Burch, D. E. and Williams, D. 1956. Near infrared transmission through synthetic atmospheres. *J. Opt. Soc. Am. 46*, 237–241.

Kiehl, J. T. and Yamanouchi, T. 1985. A parameterization for absorption due to the A, B and γ oxygen bands. *Tellus 37B*, 1–6.

Kiehl, J. T. and Ramanathan, V. 1983. CO_2 radiative parameterization used in climate models: comparison with narrow band models and laboratory data. *J. Geophys. Res. 88*, 5191–5202.

Lacis, A. A. and Hansen, J. E. 1974. A parameterization for the absorption of solar radiation in the earth's atmosphere. *J. Atmos. Sci. 31*, 118–133.

Ramanathan, V. 1976. Radiative transfer within the earth's troposphere and stratosphere: a simplified radiative-convective model. *J. Atmos. Sci. 33*, 1330–1346.

Ramanathan, V. and Dickinson, R. E. 1979. The rôle of stratospheric ozone in the zonal and seasonal radiative energy balance of the earth-troposphere system. *J. Atmos. Sci. 36*, 1084–1104.

Ramanathan, V., Pitcher, E. J., Malone, R. C. and Blackmon, M. L. 1983. The response of a spectral general circulation model to refinements in radiative processes. *J. Atmos. Sci. 40*, 605–630.

Raschke, E. and Stucke, U. 1973. Approximations of band transmission functions by finite sums of exponentials. *Beitr. Phys. Atmos. 46*, 203–212.

Rothman, L. S. and Young, L. D. G. 1981. Infrared energy levels and intensities of carbon dioxide II. *J. Quant. Spectrosc. Rad. Trans. 25*, 505–524.

Rothman, L. S., Gamache, R. R., Barbe, A., Goldman, A., Gillis, J. R., Brown, L. R., Toth, R. A., Flaud, J.-M. and Camy-Peyret, C. 1983. AFGL atmospheric absorption line parameters compilation, 1982 edition. *Appl. Opt. 22*, 2247–2256.

Sasamori, T., London, J. and Hoyt, D. V. 1972. Radiation budget of the Southern Hemisphere. *Meteorol. Monogr. 13*, 9–23.

Steinfeld, J. I. 1974. *Molecules and radiation. An Introduction to modern molecular spectroscopy*. Harper and Row, New York.

Tanaka, M. and Yamanouchi, T. 1977. Absorption properties of the near infrared CO_2 bands. *J. Quant. Spectrosc. Rad. Trans. 17*, 421–432.

Tubbs, L. D. and Williams, D. 1972. Broadening of infrared absorption lines at reduced temperatures: carbon dioxide. *J. Opt. Soc. Am. 62*, 284–289.

Vasilevskii, K. P., Danilochinka, L. E. and Kazbanov, V. A. 1975. Intensities and halfwidths of CO_2 lines in the vibrational rotational bands at 2.0 μm. *Opt. Spectrosc. (USSR) 38*, 499–500.

Wiscombe, W. J. and Evans, J. W. 1977. Exponential-sum fitting of radiative transmission functions. *J. Comp. Phys. 24*, 416–444.

Yamamoto, G. 1962. Direct absorption of solar radiation by atmospheric water vapor, carbon dioxide and molecular oxygen. *J. Atmos. Sci. 19*, 182–188.

Yamanouchi, T. 1977. Experimental study on the absorption properties of the near infrared atmospheric bands (in Japanese). D. Sc. Thesis, Tohoku Univ.